Published in final edited form as:
J Alzheimers Dis. 2010 ; 20(4): 1243–1253. doi:10.3233/JAD-2010-100210.

Differential Accumulation of Secreted APP Metabolites in Ocular Fluids

Annamalai Prakasam[1], **Anusuya Muthuswamy**[1], **Zsolt Ablonczy**[2], **Nigel H. Greig**[3], **Abdul Fauq**[4], **Kosagisharaf Jagannatha Rao**[1], **Miguel A. Pappolla**[1], and **Kumar Sambamurti**[1,*]

[1]Department of Neurosciences, Medical University of South Carolina, 173 Ashley Avenue, BSB 403, Charleston, SC 29425

[2]Department of Ophthalmology, Medical University of South Carolina, 167 Ashley Avenue, Storm Eye Institute, Rm 518, Charleston, SC 29425

[3]Laboratory of Neurosciences, Intramural Research Program, National Institute on Aging, National Institutes of Health, Baltimore, MD 21224

[4]Department of Neurosciences, Mayo Clinic, 6400 San Pablo Road, Jacksonville, FL 32224

Abstract

The Alzheimer amyloid-β (Aβ) accumulates in several types of retinal degeneration and in Alzheimer disease (AD), but its source has been unclear. We detected the neuronal 695 amino acid form of Aβ-precursor protein (AβPP) in the normal retina and AβPP751 in the retinal pigment epithelium (RPE) and anterior eye tissues. Similar to the brain, α- and β-secretases cleaved AβPP to soluble derivatives (sAPP) α or β and membrane-bound C-terminal fragments (CTF) α or β in the retina and RPE. Levels of sAPP were particularly high in the vitreous and low in aqueous humor revealing a molecular barrier for AβPP. In contrast, Aβ40 and Aβ42 levels were only 50% lower in the aqueous than the vitreous humor, indicating relatively barrier-free movement of Aβ. These studies demonstrated a relatively high yield of AβPP and Aβ in the ocular fluids, which may serve as a trackable marker for AD. In addition, failure of free clearance from the eye may trigger retina degeneration in a manner similar to Aβ-related neurodegeneration in AD.

Keywords

amyloid precursor protein; Alzheimer disease; eye vitreous humor; aqueous humor; retina; age-related macular degeneration; glaucoma; retina; degeneration

INTRODUCTION

Alzheimer disease (AD) is an extensively studied neurodegenerative disease associated with amyloid-β (Aβ) deposits in senile plaques and cerebrovascular amyloid and microtubule associated protein tau (MAPT) deposits in neurofibrillary tangles (NFT). It annually afflicts more than 4.5 million Americans and costs over $100 billion in healthcare expenses within the USA (http://www.alz.org/national/documents/report_alzfactsfigures2009.pdf; http://www.nia.nih.gov/NR/rdonlyres/0FA2EE06-0074-4C45-BAA3-34D56170EB8B/0/Unraveling_final.pdf). Several studies have provided evidence that Aβ is deposited in the eyes of patients with age-related macular degeneration (AMD), within drusen deposits

*To whom correspondence should be addressed: Kumar Sambamurti, Ph.D., Professor, Department of Neurosciences, Medical University of South Carolina, 173 Ashley Avenue, BSB 403, Charleston, SC 29425, < sambak@musc.edu>, Fax: 1-843-792-1066.

All authors declare no conflict of interest.

between the retinal pigment epithelium (RPE) and the choroidal Bruch's membrane [1–6]. Depending on the type, size, confluence, and location of the drusen, the disease can progress towards geographic atrophy and choroidal neovascularization. Aβ, a clinical biomarker in AD, is an integral component of drusen. Like senile plaques, drusen also contains deposits of apolipoprotein E (ApoE), a major risk factor for AD as well as AMD [7].

The Aβ sequence spans portions of the ectodomain and transmembrane domains of a larger type-I integral membrane Aβ protein precursor (AβPP) of 695–770 residues generated by alternative splicing of a single gene on chromosome 21 and undergoes proteolytic processing as described below [8, 9]. Most AβPP (~90%) is cleaved between residues 16 and 17 of AβPP to secreted derivative sAPPα and a membrane-bound C-terminal fragment (CTF) of 83 aa – CTFα - by an enzyme known as α-secretase. About 5–10% of AβPP is also processed by β-secretase (a.k.a. BACE-1) at the N-terminal side of Aβ to sAPPβ and a membrane-bound CTF of 99 aa (CTFβ). A multisubunit complex protease, γ-secretase, cleaves CTFα and β within their transmembrane domains to secrete the 3 kDa P3 and 4 kDa Aβ, respectively. A large body of literature suggests that Aβ aggregation, accumulation and deposition triggers the neurodegenerative cascade that leads to dementia in AD.

Recently, an animal model of AMD has been developed using a transgenic mouse model expressing the ε variant of human ApoE coupled with a high-fat diet [10]. In this model, retina degeneration was successfully treated using an anti-Aβ antibody [11]. Accordingly, it was thought that Aβ, together with related factors, could induce AMD.

Electroretinograms (ERGs) of AD patients indicate pathological changes similar to those of glaucoma, a leading cause of blindness [12, 13]. In one study of experimental glaucoma, immunohistochemistry suggests that Aβ can accumulate around retinal ganglion cells (RGCs), and anti-Aβ treatment reduces RGC apoptosis [14]. Others have developed a noninvasive diagnosis method for AD based on accumulation of Aβ in specific forms of cataract [15]. However, in all these studies, the source of Aβ remained unclear and one was left to wonder whether the paper-thin retinal tissue could generate sufficient Aβ to induce damage and eventual neurodegeneration. Therefore, a systematic investigation of AβPP changes in various ocular tissues associated with environmental and genetic risk factors is critical to elucidate the pathogenesis of both AMD and glaucoma. With the ocular tissues being easily accessible, data gathered from studies using the eye as a model may also prove to be useful for understanding protein accumulation in the brain. In this study, we characterized the dynamics of AβPP metabolism in the eye under normal conditions, to set the standards for future studies on the role of AβPP in retina and central nervous system degeneration.

MATERIALS AND METHODS

Chemicals, antibodies, and standard peptides

All chemicals were purchased in the highest purity available (analytical or molecular, biological grade), unless stated otherwise. The γ-secretase inhibitor, LY411575, was custom synthesized at the Mayo Clinic chemistry core facility [16].

The rabbit antibody O443 against the C-terminal 20 residues of AβPP (CKMQQNGYENPTYKFFEQMQN) and the anti-PS1 antibody against residues 2–13 (CRKTELPAPLSYF) were as described previously [17, 18]. The R7 antibody against the Kunitz protease inhibitor (KPI) domain of AβPP was a gift from Dr. Nikolaos Robakis [19]. Other antibodies used were obtained from several sources as follows: monoclonal 6E10 (against residues 1–17 of Aβ, Covance, Emeryville, CA, USA), 22C11 (N-terminal 66–81 aa of AβPP, Boehringer Mannheim, GmbH Germany), anti-human BACE-1 (Abcam 23796

against recombinant BACE-1; Abcam2077 against residues 485–501), anti-PEN-2 (Zymed, CA, USA), anti-Nicastrin (Cell Signaling, Danvers, MA, USA), anti-APH1a (Abcam, Cambridge, UK) and peroxide-conjugated secondary antibodies (Jackson ImmunoResearch (West Grove, PA, USA).

The LC99 construct consisting of the signal sequence of AβPP fused to its C-terminal 99 residues was expressed in Chinese hamster ovary (CHO) cells and used as a standard for C-terminal fragment β (CTFβ) [20]. CHO-2B7 cells (a gift from Todd Golde, Mayo Clinic, Jacksonville, FL, USA) expressing wild type AβPP695 were used as a standard for CTFα and AβPP.

ELISA kits for Aβ40 (IBL Co. Ltd, Gunma, Japan) and Aβ42 (Innogenetics, Gent, Belgium) were used for the analysis of Aβ. These kits were subjected to multiple validation tests including lack of cross reactivity with full-length AβPP and other Aβ-like fragments. However, they still showed low levels of nonspecific reactivity based on the samples measured. To ensure specificity, we included a competition with the Aβ1–16 peptide with detection antibody for each sample tested in the assay and subtracted the nonspecific reactivity before calculating the values.

Animals

All animal procedures were approved and supervised by the Institutional Animal Care and Use Committee of the Medical University of South Carolina and adhered to the tenets of the Declaration of Helsinki and the ARVO Statement for the Use of Animals in Ophthalmic and Vision Research. BALB/c mice were obtained from the Jackson Laboratory (Bar Harbor, ME, USA) and maintained in a 12-hour light/dark cycle. BACE-1 knockout mice and AβPP-PS1 transgenic mice were obtained from the Jackson laboratory. Over-expressing AβPP mice (AβPP-YAC), generated under the yeast artificial chromosome [21], were gifts from Bruce Lamb (Department of Genetics, Case Western Reserve University, Cleveland, OH, USA). AβPP knock-out mice (AβPP-KO) were gifts from Dr. Hui Zheng (Huffington Center on Aging, Baylor College of Medicine, Houston, TX, USA). One- to three-month-old mice were used for the experiments. Bovine eyes were obtained on dry ice from Cocalico Biologicals, Inc. (Reamstown, PA, USA).

Eye dissection and tissue isolation

Eyes (bovine and mice) were enucleated and dissected to obtain the retina (RET), RPE, aqueous humor (AQE), and vitreous humor (VIT). The anterior segment of the eye was removed using a fine scissor with a circumferential cut behind the limbus to release the cornea. Aqueous humor was collected from the center of the cornea using a disposable plastic syringe. A 26 gauge needle (through the corneal edge) was used to collect vitreous humor. The whole eye was then cut into two, equal hemispheres and the retina was carefully removed. The lens was removed from the anterior cup and the lens epithelium was dissected. The RPE was removed from the interior surface of the posterior globe under a dissecting microscope by repetitive brushing in the presence of PBS. Since mouse eyes are very small, they were supported within small wells drilled into a plexiglass sheet under the microscope (Nikon SMZ 800, Japan). All ocular tissue collections were immediately frozen on dry ice and stored at −80°C until analysis.

Biochemical analysis

Dissected tissues were homogenized using a high-speed tissue homogenizer (PRO Scientific, Oxford, CT, USA) and 10 volumes of homogenization buffer (10 mM HEPES, pH7.4; 1 mM EDTA, 0.25 M sucrose + 5 mM o-phenanthroline and protease-inhibitor cocktail; Sigma-Aldrich CO. St Louis, MO, USA). Total membrane pellets were obtained by

centrifugation in a Sorvall RCM100 microultracentrifuge for 60 min at 100,000*g* and analyzed by Western blotting as described previously, with the exception that the signal was detected using a chemiluminescence detector (Fluorchem HD, Alpha Innotech, Santa Clara, CA, USA) [17].

Aβ was analyzed using ELISA kits obtained from IBL (Aβ40) and Innogenetics (Aβ42) and the assay carried out according to manufacturer's instructions, with a few key modifications. The major modification in the Aβ40 assay was the replacement of its detection antibody and other detection reagents with the same reagents from the Innogenetics kit to reduce background. Nonspecific immunoreactivity was determined and subtracted for each sample after competition of the detection antibody with the Aβ1–16 peptide.

In vivo studies

To analyze the effect of cycloheximide (CXM) on AβPP metabolism, non-transgenic wild-type BALB/c mice were used at 8–10 weeks-of-age (body weight 26.2 ± 2.3 g), and groups of mice intraperitoneally-injected with either saline or 6 mg/kg CXM. Four mice were dissected at each indicated time point (0.5, 1, 2, 4 hours) post-treatment and analyzed as described earlier.

γ-Secretase activity was inhibited in transgenic mice over-expressing the human *AβPP* gene with the Swedish double-mutation mice, K670N/M671L, under the control of the Yeast Artificial Chromosome [21] by intraperitoneal injection of a potent γ-secretase inhibitor, LY411575, in 3 mg/kg in corn oil as reported previously [22]. Mice for this study were fasted overnight, treated in groups of 4 for 8 hours or 12 hours, euthanized in a CO_2-saturated chamber followed by decapitation. The animals were dissected under a microscope to obtain the RPE and other retina tissue and brain for further analysis, as described earlier.

RESULTS

AβPP is expressed in the retina and the RPE

To identify the ocular tissue in which AβPP is expressed, the cornea, retina, RPE, aqueous humor, vitreous humor, iris, and lens were analyzed from bovine eyes (Fig. 1A, E). The retina (Fig. 1B), RPE (Fig. 1C), and vitreous humor (Fig. 1F, 1G) from bovine and murine eyes, were also compared. Western blotting utilized the O443 antibody against the last 20 amino acids (aa) of AβPP (Fig. 1A–D), 6E10 against Aβ1–16 (Fig. 1E), 22C11 against AβPP ectodomain (61–81 aa; Fig. 1F), and 10D1 end-specific for sAPPβ (Fig. 1G). Brains from AβPP transgenic mice were used as positive controls (Fig. 1D). To identify the specific AβPP bands, we included knockout mouse controls and competition assays (Fig. 2).

The O443 antibody detects full-length AβPP of 110–130 kDa in the cornea, retina, RPE, iris and vitreous humor, but not in the lens and aqueous humor (Fig. 1A). The migration pattern on polyacrylamide gels is consistent with a mix of mature and core glycosylated AβPP695 (695 aa) that are characteristic of neurons in the retina (Fig. 1A) [17]. The longer KPI domain-bearing AβPP751 is seen in the cornea, RPE and iris (Figs. 1A, 2). Similar AβPP patterns were found in the murine retina (Fig. 1B) and RPE (Fig. 1C) as well. C-terminal fragments (CTFs) of ~11 kDa, generated predominantly by α-secretase, were observed both in the retina and RPE (Fig. 1A–C), but not in the other tissues. Additional bands detected between 14 and 110 kDa persist after competition and are also seen in AβPP-KO mice suggesting that they are nonspecific, and were therefore ignored (Fig. 2).

Previous studies have reported significant levels of AβPP in the lens and have attributed its presence to cataract formation [23–25]. We were unable to detect AβPP in the normal adult

bovine lens lysate (Fig. 1A, E). Further studies using eyes from cataract patients are needed to confirm and understand the cause of Aβ accumulation.

Secreted-AβPP accumulates in the vitreous humor

The bovine eye tissues listed above were probed with the 6E10 antibody to detect α-secretase-cleaved AβPP that forms soluble (sAPPα) (Fig. 1E). Although this antibody can also detect full-length AβPP, the relative increase in band intensity in the aqueous and vitreous humors compared to the other tissues suggests that it is the cleaved and secreted product, sAPPα, which lacks the intracellular domain required for O443 reactivity. Since 6E10 does not detect mouse AβPP, we demonstrated the presence of total sAPP in the mouse vitreous humor with 22C11 against residues 66–81 from the N-terminus of AβPP (Fig. 1F). In addition, sAPPβ derived by BACE-1 cleavage was also detected in the vitreous humor (Fig. 1G).

The overwhelmingly high levels of sAPPα in the vitreous humor (Fig. 1E) is comparable only to that found in the cerebrospinal fluid (CSF; Annamalai and Sambamurti, 2005, unpublished observations). As the tissues surrounding the vitreous humor, including the retina, are very thin and of low volume, the presence of this large a quantity of sAPPα in the vitreous suggests that its clearance is very slow, leading to an accumulation of sAPPα. Some sAPPα is also seen in the aqueous humor (Fig. 1E), but its levels are orders of magnitude lower, suggesting that the protein is unable to efficiently diffuse across the hyaloid membrane that separate the two humors [26].

The retina secretes most of the sAPP detected in aqueous and vitreous humors

Since large amounts of sAPPα and sAPPβ are found in the vitreous humor (Fig. 1), it is important to identify their source. Is the neural retina responsible for most of the sAPP or is it derived predominantly from other tissues in the eye? To identify the type of AβPP within the eye, we biased the gel system to increase separation at the higher size range and compared the bands detected by 6E10 with a second antibody R7 (Fig. 3), raised against portions of the KPI domain in AβPP751 [19].

The 6E10 antibody detects a major band of 110 kDa and a relatively minor band of 120 kDa in the vitreous and aqueous humors (Fig. 3A). The R7 antibody detects a larger 120 kDa band (Fig. 3B) that co-migrates with the minor 120 kDa sAPPα band detected by 6E10 in the vitreous and aqueous humor lanes and shown in Fig. 3A. R7, however, does not detect the major smaller 110 kDa sAPPα band in the aqueous and vitreous humors. Since the intensity of the 120 kDa KPI-containing band detected by 6E10 is faint compared to the 110 kDa band, most sAPP is derived from the neuronal form, AβPP695, and therefore from the retina. Earlier, we noted that the retinal AβPP is smaller than in other eye tissues, including the RPE (Fig 1). However, the RPE layer surrounding the retinal tissue showed two bands. One of these bands is larger while the other migrates with the retinal AβPP695. The smaller band could either be the core glycosylated form of AβPP751 containing the KPI domain or AβPP695. To distinguish between these possibilities, we measured AβPP in primary porcine RPE cells and a human RPE cell line (ARPE-19). Both O443 (Fig 3C) and R7 (Fig 3D) detected both AβPP bands showing that they contain the KPI domain seen in AβPP751. Therefore, unlike the retina, little or no AβPP695 is expressed in RPE cells.

Interestingly, a large fraction of the sAPP in aqueous humor is also derived from AβPP695 (Fig. 3A, AQE). As the surrounding tissues express predominantly AβPP751, this finding suggests that sAPP diffuses from the vitreous into the aqueous humor. However, the large difference in the concentration of sAPPα in the vitreous and aqueous humors suggest that either this transfer is fairly inefficient or that the protein is rapidly cleared from the aqueous

humor. This result is surprising, because most of the studies on fluid dynamics in the eye would suggest that the flow should be in the other direction (i.e., from the aqueous to the vitreous and on toward the choroid via the RPE [27]). However, consistent with our findings, one report shows that the flow can occur in both directions [28]. Moreover, the tight RPE barrier does not normally allow the clearance of peptides and proteins.

Our study of the retina and RPE, demonstrate that AβPP is processed by the major α- and β-secretase pathways previously identified in the brain and suggest that a pathway exists for the clearance of sAPPα via the anterior eye chamber, although this is a slow and inefficient route based on the large accumulation of this protein in the vitreous humor. Additional studies are needed to understand the clearance pathways for sAPPα from the closed vitreous humor system which will provide valuable information on the causes of protein accumulation with age. The fate of secreted AβPP derivatives is a poorly understood area of study even in the brain, as most of the focus has been on Aβ42 and its potential toxicity in AD. This is likely to change with the discovery of a toxic fragment derived from the AβPP ectodomain, termed N-APP [29].

AβPP is rapidly turned over in the eye and in the brain

To understand AβPP turnover rates *in vivo*, total protein synthesis was inhibited with a single intraperitoneal injection of CXM (6 mg/kg) in mice, and tissue was collected at 0.5, 1, 2 and 4 hours after treatment. Levels of AβPP and CTFα in both the retina (Fig. 4A) and the RPE (Fig. 4B) dropped rapidly (0.5 hours) and remained low for 4 hours (Fig. 4C–D). Both cortices (CTX) and hippocampi (data not shown) extracted from the same mice showed a more gradual, but sustained reduction in AβPP and CTFα. The simplest conclusion from these studies is that the protein synthesis inhibitor, CXM, diffuses into the eyes more rapidly than the brain, but one cannot rule out the possibility that AβPP is even more rapidly turned over in the retina and RPE than in the brain. Regardless of the details, however, the data show that AβPP is rapidly metabolized *in vivo* by α- and β-secretase in the eye and the brain, as in neuronal cells in culture [19].

Retina and RPE cells express all the factors necessary for Aβ production

Retina and RPE cells were dissected from mouse eyes and analyzed for the presence of BACE-1 and the four known subunits of γ-secretase (PS1, Aph-1, Pen-2, and NCT) by Western blotting. Transformed CHO cells and brain from normal and BACE-1 knockout mice served as controls. A 70 kDa BACE-1 immunoreactive band is observed in all tissues except in BACE-1 knockout mouse brain (Fig. 5A). BACE-1 immunoreactivity was higher in the RPE than in the retina, but the protein is normally preferentially expressed in neurons in the brain. The reason for this discrepancy is not clear, but it is a consistent finding in mice. Since RPE cells continuously phagocytose retinal membranes for their maintenance, it is possible that some of the signal arises from retinal membranes. PS1, Aph-1, Pen-2 and NCT were expressed in all studied tissues (Fig. 5B–E), demonstrating that both the retina and the RPE possess all the components necessary for Aβ production.

CTFs from AβPP are processed by γ-secretase in the eye

The CTFα and CTFβ fragments generated by α- and β-secretase cleavage of AβPP are further processed by γ-secretase to generate Aβ and a 3 kDa fragment (P3) in the brain [8]. LY411575 (γ-secretase inhibitor, 3 mg/kg) treatment of mice expressing the entire AβPP gene in a yeast artificial chromosome with a familial AD (FAD) mutation (KM670NL) for 8 or 12 hours, increased the levels of both CTFα and CTFβ in the retina (Fig. 6A–B), RPE (Fig. 6C–D), and brain (Fig. 6E–F) demonstrating that all the major AβPP processing pathways described in the brain are active in the retina and the RPE. AβPP levels remain constant during this treatment showing that its synthesis and turnover by the α- and β-

secretase pathways are rapid and not affected by the inhibition of γ-secretase in the brain and the eye.

The KM670NL mutant form of AβPP is a better substrate for β-secretase, and therefore yields higher levels of CTFβ and Aβ [8]. Consistently, relative to CTFα, the brains of these mice show high levels of CTFβ (Fig. 6E–F). However, CTFβ levels in the retina (Fig. 6A–B) and RPE cells (Fig. 6C–D) remain relatively low, suggesting that β-secretase processing is less efficient in the retina and RPE than the brain and may consequentially yield lower levels of Aβ than the brain.

Both Aβ40 and Aβ42 are present in the aqueous and vitreous humors

Using sensitive commercial Aβ ELISA kits (Innogenetics and IBL America), we measured the levels of Aβ40 and Aβ42 in the various eye tissues from bovine and transgenic mice. Aβ was not detected in the retina and RPE (data not shown). These data are consistent with other recent reports [30]. On the other hand, significant amounts of Aβ40 and Aβ42 were detected in the aqueous and vitreous humors of all the models tested (Fig. 7). We had a similar observation in the brain, where Aβ levels are normally low, as it is secreted and mostly concentrated in the CSF (Annamalai and Sambamurti, 2005, unpublished observation). Moreover, in the eye, the vitreous consistently showed higher levels of Aβ than the aqueous humor. As sAPP appears to be produced in the retina, secreted into the vitreous humor and transported into the aqueous humor, we conclude that Aβ follows the same path. However, unlike sAPP, Aβ40 and Aβ42 levels are only marginally higher in the vitreous humor than the aqueous humor. We therefore conclude that the hyaloid membrane barrier between the aqueous and vitreous humors does not permit easy access to large proteins, such as sAPPα, but is sufficiently permeable to permit diffusion of a small peptide like Aβ. Aβ is reported to be rapidly transported from the brain into the circulation using the low-density lipoprotein receptor-related protein (LRP) [31]. Additionally, the multi-drug resistance, or P-glycoprotein pathway, has been identified as an Aβ transporter [32]. It is possible that the transport of Aβ from the vitreous to the aqueous humor depends on the activity of one or more such transporters, instead of passive diffusion, and may therefore not be size-limited.

DISCUSSION

AβPP is a highly expressed protein within the nervous system with a short half-life of about 20 min, at least such is the case in cell culture [9, 19]. Its mismetabolism leads to accumulation of Aβ42, which aggregates to yield oligomers that are generally considered the trigger in AD pathogenesis [33]. A number of studies suggest that several forms of retinal degeneration including AMD and glaucoma are associated with increases in Aβ and may be triggered by its toxicity. Despite the critical nature of this information, the presence of AβPP and its metabolism to Aβ has not been systematically studied in the eye. One exception is a report showing that Aβ42 is greatly reduced and MAPT is increased in the vitreous humor and CSF of AD patients [34].

In addition to demonstrating that AβPP is expressed and secreted from the retina and RPE cells into the vitreous humor, our studies demonstrate that a molecular barrier exists between the aqueous and vitreous humors. This barrier ensures that sAPP levels in the aqueous humor are low, but Aβ remains high, which should allow its rapid clearance from the eye via Schlemm's canal. Thus, the aqueous humor may be a valuable sampling location that can identify genetically- and epigenetically-induced increases in Aβ42 characteristic of FAD mutations, or reductions in Aβ in the CNS in response to treatments.

Although the collection of ocular fluids raises concern for safety and acceptance, eyes have been safely tapped for a number of ocular treatments (e.g., [35–37]). In addition, there are patents for the diagnosis of AD based on the activity of acetylcholinesterase activity in ocular fluids [38]. Albeit, Aβ levels are lower in ocular fluids than in the CSF, they do not show a high level of variance making them stable markers for analyses. In addition the rapid turnover of ocular fluids would imply by extension, that Aβ might allow superior measurement for detection of Aβ changes after treatment with drugs. In clinical studies of the γ-secretase inhibitor, LY450139, which inhibits Aβ production at the last and, arguably the most sensitive step in its generation, reduced plasma Aβ without affecting CSF Aβ levels. This response likely developed due to the large available pool and slow turnover of CSF [39]. In contrast, as the vitreous humor is in direct contact with a large part of the retina, it can be expected to directly reflect changes in Aβ production in this part of the CNS.

Since Aβ appears to accumulate and deposit in some forms of retinal degeneration, such as AMD and glaucoma, these patients may benefit from treatment with anti-amyloid drugs developed for AD. It will also be important to identify the transport pathways for Aβ from the vitreous to the aqueous humors. Given that the ocular chambers are readily accessible, the eye may lead to a better understanding of the pathways leading to Aβ accumulation and aggregation in the CNS. Such studies may also explain some of the differences in the epidemiology of AD and AMD [7].

The presence of the AβPP pathway within the eye supports the notion that it may form the basis for degenerative diseases, such as AMD and glaucoma, and can explain the abnormal neurons reported in the eyes of AD patients [40]. It is critical to evaluate the changes in human disease by a careful analysis of Aβ, AβPP, ApoE, MAPT and related proteins in the aqueous and vitreous humors to understand their role in neurodegeneration. Finally, our study suggests that aqueous humor proteomics focused on small peptide metabolites may prove of considerable value for development of diagnostic systems for diseases of the retina and the central nervous system, in general.

Acknowledgments

Supported in part by NIH grants AG028544, AG023055 (K.S.); NIH, IRP, NIA, (N.H.G.); and the American Health Assistance Foundation (KS). The authors would like to thank Peter Chung, Corey Snelson, Laura Marlow and Dr. Sharie Haugabook for some of the initial characterization studies; and Meera Parasuraman, Lucy Feingold for their help in preparing the manuscript, and Dr. Luanna Bartholomew for critical review.

References

1. Anderson DH, Talaga KC, Rivest AJ, Barron E, Hageman GS, Johnson LV. Characterization of beta amyloid assemblies in drusen: the deposits associated with aging and age-related macular degeneration. Exp Eye Res. 2004; 78:243–256. [PubMed: 14729357]
2. Dentchev T, Milam AH, Lee VM, Trojanowski JQ, Dunaief JL. Amyloid-beta is found in drusen from some age-related macular degeneration retinas, but not in drusen from normal retinas. Mol Vis. 2003; 9:184–190. [PubMed: 12764254]
3. Luibl V, Isas JM, Kayed R, Glabe CG, Langen R, Chen J. Drusen deposits associated with aging and age-related macular degeneration contain nonfibrillar amyloid oligomers. J Clin Invest. 2006; 116:378–385. [PubMed: 16453022]
4. Ning A, Cui J, To E, Ashe KH, Matsubara J. Amyloid-beta deposits lead to retinal degeneration in a mouse model of Alzheimer disease. Invest Ophthalmol Vis Sci. 2008; 49:5136–5143. [PubMed: 18566467]

5. Perez SE, Lumayag S, Kovacs B, Mufson EJ, Xu S. Beta-amyloid deposition and functional impairment in the retina of the APPswe/PS1DeltaE9 transgenic mouse model of Alzheimer's disease. Invest Ophthalmol Vis Sci. 2009; 50:793–800. [PubMed: 18791173]
6. Yoshida T, Ohno-Matsui K, Ichinose S, Sato T, Iwata N, Saido TC, Hisatomi T, Mochizuki M, Morita I. The potential role of amyloid beta in the pathogenesis of age-related macular degeneration. J Clin Invest. 2005; 115:2793–2800. [PubMed: 16167083]
7. Prakasam, A.; Venugopal, C.; Suram, A.; Pacheco-Quinto, J.; PMA; Sharpe, KA.; Lahiri, DK.; Greig, NH.; Rohrer, B.; Sambamurti, K. Amyloid and neurodegeneration: Alzheimer's disease and retinal degeneration. In: Banik, NaRSK., editor. Handbook of Neurochemistry and Molecular Neurobiology: Brain and Spinal Chord Trauma. Springer; New York: 2008. p. 131-163.
8. Sambamurti K, Greig NH, Lahiri DK. Advances in the cellular and molecular biology of the beta-amyloid protein in Alzheimer's disease. Neuromolecular Med. 2002; 1:1–31. [PubMed: 12025813]
9. Sambamurti K, Suram A, Venugopal C, Prakasam A, Zhou Y, Lahiri DK, Greig NH. A partial failure of membrane protein turnover may cause Alzheimer's disease: a new hypothesis. Curr Alzheimer Res. 2006; 3:81–90. [PubMed: 16472208]
10. Malek G, Johnson LV, Mace BE, Saloupis P, Schmechel DE, Rickman DW, Toth CA, Sullivan PM, Bowes Rickman C. Apolipoprotein E allele-dependent pathogenesis: a model for age-related retinal degeneration. Proc Natl Acad Sci U S A. 2005; 102:11900–11905. [PubMed: 16079201]
11. Ding JD, Lin J, Mace BE, Herrmann R, Sullivan P, Bowes Rickman C. Targeting age-related macular degeneration with Alzheimer's disease based immunotherapies: anti-amyloid-beta antibody attenuates pathologies in an age-related macular degeneration mouse model. Vision Res. 2008; 48:339–345. [PubMed: 17888483]
12. Bayer AU, Keller ON, Ferrari F, Maag KP. Association of glaucoma with neurodegenerative diseases with apoptotic cell death: Alzheimer's disease and Parkinson's disease. Am J Ophthalmol. 2002; 133:135–137. [PubMed: 11755850]
13. Nesher R, Trick GL. The pattern electroretinogram in retinal and optic nerve disease. A quantitative comparison of the pattern of visual dysfunction. Doc Ophthalmol. 1991; 77:225–235. [PubMed: 1760971]
14. Guo L, Salt TE, Luong V, Wood N, Cheung W, Maass A, Ferrari G, Russo-Marie F, Sillito AM, Cheetham ME, Moss SE, Fitzke FW, Cordeiro MF. Targeting amyloid-beta in glaucoma treatment. Proc Natl Acad Sci U S A. 2007; 104:13444–13449. [PubMed: 17684098]
15. Goldstein LE, Muffat JA, Cherny RA, Moir RD, Ericsson MH, Huang X, Mavros C, Coccia JA, Faget KY, Fitch KA, Masters CL, Tanzi RE, Chylack LT Jr, Bush AI. Cytosolic beta-amyloid deposition and supranuclear cataracts in lenses from people with Alzheimer's disease. Lancet. 2003; 361:1258–1265. [PubMed: 12699953]
16. Fauq AH, Simpson K, Maharvi GM, Golde T, Das P. A multigram chemical synthesis of the gamma-secretase inhibitor LY411575 and its diastereoisomers. Bioorg Med Chem Lett. 2007; 17:6392–6395. [PubMed: 17897827]
17. Pinnix I, Musunuru U, Tun H, Sridharan A, Golde T, Eckman C, Ziani-Cherif C, Onstead L, Sambamurti K. A novel gamma-secretase assay based on detection of the putative C-terminal fragment-gamma of amyloid beta protein precursor. J Biol Chem. 2001; 276:481–487. [PubMed: 11035007]
18. Duff K, Eckman C, Zehr C, Yu X, Prada CM, Perez-tur J, Hutton M, Buee L, Harigaya Y, Yager D, Morgan D, Gordon MN, Holcomb L, Refolo L, Zenk B, Hardy J, Younkin S. Increased amyloid-beta42(43) in brains of mice expressing mutant presenilin 1. Nature. 1996; 383:710–713. [PubMed: 8878479]
19. Sambamurti K, Shioi J, Anderson JP, Pappolla MA, Robakis NK. Evidence for intracellular cleavage of the Alzheimer's amyloid precursor in PC12 cells. J Neurosci Res. 1992; 33:319–329. [PubMed: 1453494]
20. Golde TE, Estus S, Younkin LH, Selkoe DJ, Younkin SG. Processing of the amyloid protein precursor to potentially amyloidogenic derivatives. Science. 1992; 255:728–730. [PubMed: 1738847]

21. Lamb BT, Sisodia SS, Lawler AM, Slunt HH, Kitt CA, Kearns WG, Pearson PL, Price DL, Gearhart JD. Introduction and expression of the 400 kilobase amyloid precursor protein gene in transgenic mice [corrected]. Nat Genet. 1993; 5:22–30. [PubMed: 8220418]
22. Dovey HF, John V, Anderson JP, Chen LZ, de Saint Andrieu P, Fang LY, Freedman SB, Folmer B, Goldbach E, Holsztynska EJ, Hu KL, Johnson-Wood KL, Kennedy SL, Kholodenko D, Knops JE, Latimer LH, Lee M, Liao Z, Lieberburg IM, Motter RN, Mutter LC, Nietz J, Quinn KP, Sacchi KL, Seubert PA, Shopp GM, Thorsett ED, Tung JS, Wu J, Yang S, Yin CT, Schenk DB, May PC, Altstiel LD, Bender MH, Boggs LN, Britton TC, Clemens JC, Czilli DL, Dieckman-McGinty DK, Droste JJ, Fuson KS, Gitter BD, Hyslop PA, Johnstone EM, Li WY, Little SP, Mabry TE, Miller FD, Audia JE. Functional gamma-secretase inhibitors reduce beta-amyloid peptide levels in brain. J Neurochem. 2001; 76:173–181. [PubMed: 11145990]
23. Frederikse PH, Ren XO. Lens defects and age-related fiber cell degeneration in a mouse model of increased AbetaPP gene dosage in Down syndrome. Am J Pathol. 2002; 161:1985–1990. [PubMed: 12466113]
24. Li G, Percontino L, Sun Q, Qazi AS, Frederikse PH. Beta-amyloid secretases and beta-amloid degrading enzyme expression in lens. Mol Vis. 2003; 9:179–183. [PubMed: 12740567]
25. Perez RG, Soriano S, Hayes JD, Ostaszewski B, Xia W, Selkoe DJ, Chen X, Stokin GB, Koo EH. Mutagenesis identifies new signals for beta-amyloid precursor protein endocytosis, turnover, and the generation of secreted fragments, including Abeta42. J Biol Chem. 1999; 274:18851–18856. [PubMed: 10383380]
26. Ozaki L. The barrier function of the posterior capsule. J Am Intraocul Implant Soc. 1984; 10:182–184. [PubMed: 6588049]
27. Camelo S, Shanley AC, Voon AS, McMenamin PG. An intravital and confocal microscopic study of the distribution of intracameral antigen in the aqueous outflow pathways and limbus of the rat eye. Exp Eye Res. 2004; 79:455–464. [PubMed: 15381030]
28. Araie M, Maurice DM. The loss of fluorescein, fluorescein glucuronide and fluorescein isothiocyanate dextran from the vitreous by the anterior and retinal pathways. Exp Eye Res. 1991; 52:27–39. [PubMed: 1714398]
29. Nikolaev A, McLaughlin T, O'Leary DD, Tessier-Lavigne M. APP binds DR6 to trigger axon pruning and neuron death via distinct caspases. Nature. 2009; 457:981–989. [PubMed: 19225519]
30. Dutescu RM, Li QX, Crowston J, Masters CL, Baird PN, Culvenor JG. Amyloid precursor protein processing and retinal pathology in mouse models of Alzheimer's disease. Graefes Arch Clin Exp Ophthalmol. 2009; 247:1213–1221. [PubMed: 19271231]
31. Deane R, Bell RD, Sagare A, Zlokovic BV. Clearance of amyloid-beta peptide across the blood-brain barrier: implication for therapies in Alzheimer's disease. CNS Neurol Disord Drug Targets. 2009; 8:16–30. [PubMed: 19275634]
32. Deane R, Zlokovic BV. Role of the blood-brain barrier in the pathogenesis of Alzheimer's disease. Curr Alzheimer Res. 2007; 4:191–197. [PubMed: 17430246]
33. Hardy J. Has the amyloid cascade hypothesis for Alzheimer's disease been proved? Curr Alzheimer Res. 2006; 3:71–73. [PubMed: 16472206]
34. Yoneda S, Hara H, Hirata A, Fukushima M, Inomata Y, Tanihara H. Vitreous fluid levels of beta-amyloid((1–42)) and tau in patients with retinal diseases. Jpn J Ophthalmol. 2005; 49:106–108. [PubMed: 15838725]
35. Razonable RR, Pulido JS, Deziel PJ, Dev S, Salomao DR, Walker RC. Chorioretinitis and vitreitis due to Tropheryma whipplei after transplantation: case report and review. Transpl Infect Dis. 2008; 10:413–418. [PubMed: 18564981]
36. Funatsu H, Yamashita T, Yamashita H. Vitreous fluid biomarkers. Adv Clin Chem. 2006; 42:111–166. [PubMed: 17131626]
37. Nayak N. Fungal infections of the eye--laboratory diagnosis and treatment. Nepal Med Coll J. 2008; 10:48–63. [PubMed: 18700633]
38. Appleyard, ME.; McDonald, B. USPTO.GOV. E. R. Squibb & Sons, Inc; Princeton, NJ: 1990.
39. Siemers ER, Dean RA, Friedrich S, Ferguson-Sells L, Gonzales C, Farlow MR, May PC. Safety, tolerability, and effects on plasma and cerebrospinal fluid amyloid-beta after inhibition of gamma-secretase. Clin Neuropharmacol. 2007; 30:317–325. [PubMed: 18090456]

40. Berisha F, Feke GT, Trempe CL, McMeel JW, Schepens CL. Retinal abnormalities in early Alzheimer's disease. Invest Ophthalmol Vis Sci. 2007; 48:2285–2289. [PubMed: 17460292]

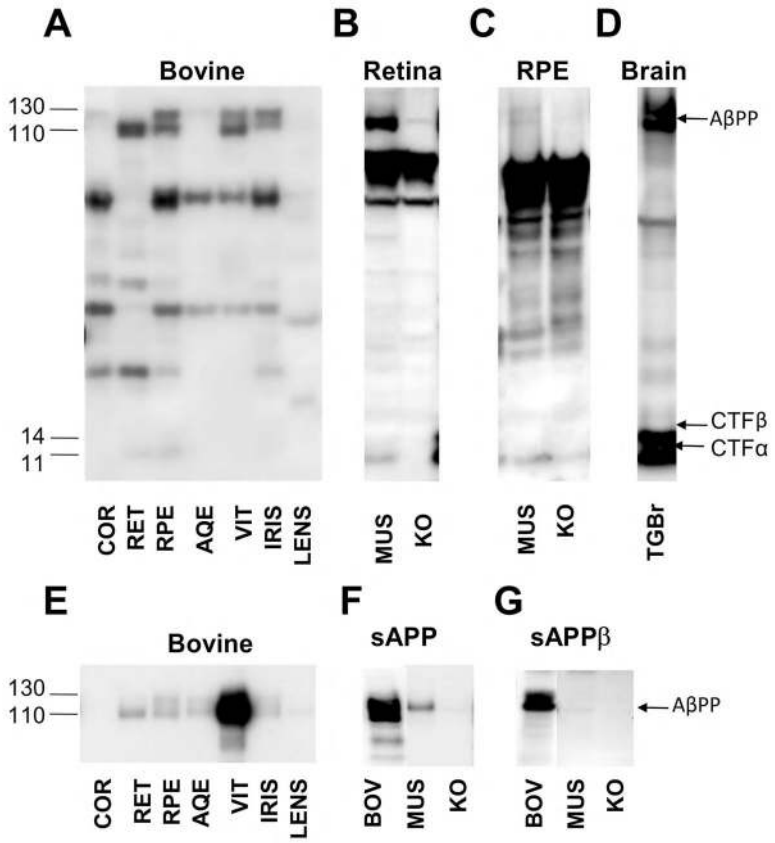

Figure 1. AβPP and its metabolites are regionally expressed in the eye

Bovine eyes were dissected to obtain the cornea (COR), retina (RET), retinal pigment epithelium (RPE), iris, aqueous humor (AQE), vitreous humor (VIT), and lens were analyzed by Western blotting with the O443 antibody to detect full length AβPP and CTFs (**A**–**D**), 6E10 against Aβ 1–16 aa in various bovine tissues (**E**) or 22C11 against AβPP 61–81 aa (**F**) to detect full-length AβPP and sAPPα, and 10D5 specific for sAPPβ (**G**) in vitreous humor samples. Bovine (BOV), murine (MUS) and AβPP knockout mouse (KO) tissues were utilized. Although murine eyes are small and difficult to digest, it is an important genetically tractable model system and was therefore also tested. Brains from AβPP-PS1 transgenic mice were used as positive controls (TGBr; **D**). Please note that the lane labels are the same in all subsequent figures.

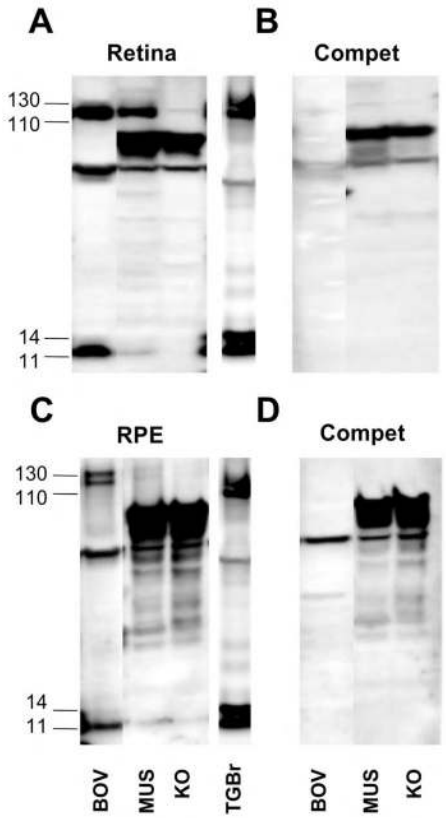

Figure 2. Competition and KO mice identify the genuine AβPP bands in retina and RPE

Bovine, wild type murine (MUC), and AβPP knockout murine (KO) retina (**A**, **B**) and retinal pigment epithelium (RPE) (**C**, **D**) were analyzed by Western blotting with O443 (**A**, **C**) or O443 preabsorbed with a peptide corresponding to the C-terminal 50 residues of AβPP (**B**, **D**). Note that bands in the 110–130 kDa and the 11–14 kDa range comigrate with similar bands in brain extracts and are lost upon peptide preabsorption. Brains from AβPP-PS1 transgenic mice were used as positive controls (TGBr)

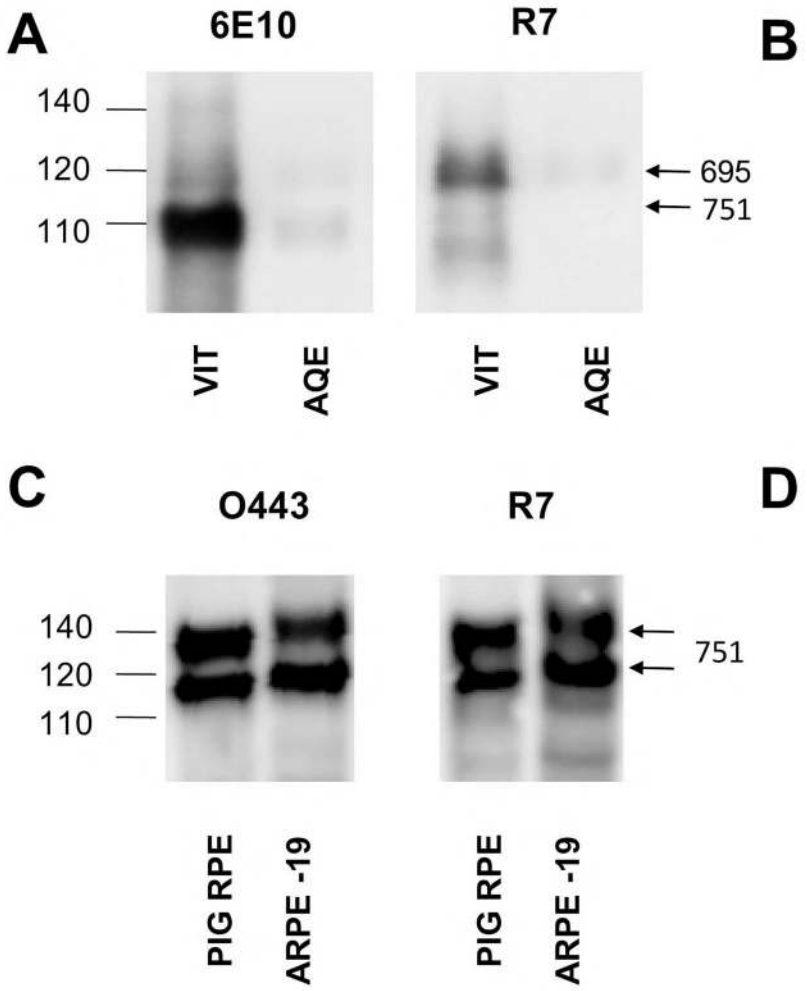

Figure 3. The predominant AβPP in the vitreous humor is the neuronal AβPP695 form

AβPP in the aqueous (AQE) and vitreous (VIT) humors, retina (RET), and retinal pigment epithelium (RPE) were compared by Western blotting with the 6E10 antibody against the Aβ1–16 sequence (**A**) and R7 against the KPI domain absent in AβPP695 (**B**). Note the absence of the major sAPP band corresponding to AβPP695 in panel B with R7. R7 does detect a minor smaller band in the vitreous humor, but this protein migrates slightly faster than the major sAPPα - AβPP695 band detected by 6E10 in panel A and is relatively fainter than the 120-kDa sAPPα - AβPP751. To determine whether RPE cells express any AβPP695, we compared the AβPP bands in porcine RPE cells and the human ARPE-19 cell line with O443 to detect all AβPP forms and R7 to detect the KPI-containing AβPP751.

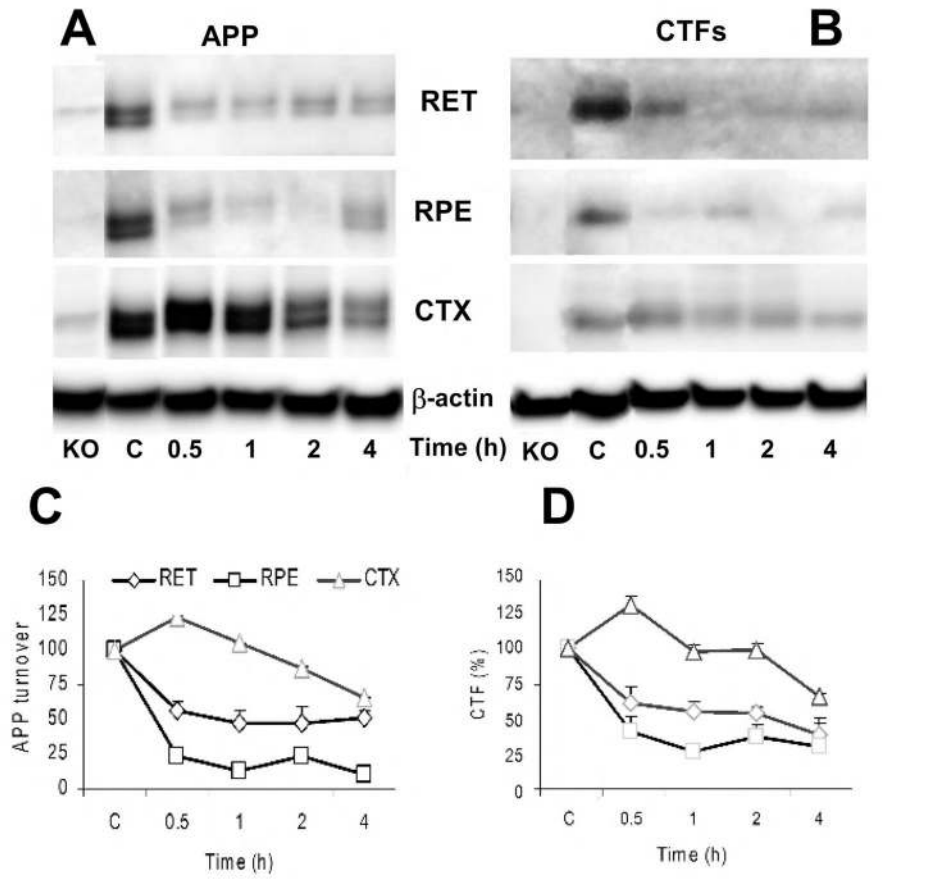

Figure 4. AβPP and CTFs are rapidly turned over in the eye and the brain

Nontransgenic BALBc mice (10–12 weeks) were administered saline (C) or cycloheximide and the tissues were collected at the indicated time post administration. Tissues from AβPP knockout mice (KO) were included as controls. Retina (RET), retinal pigment epithelium (RPE), and cortex (CTX) samples were analyzed by Western blotting with O443 antibody to detect full length AβPP (**A**) and CTFs (**B**). The AβPP (**C**) and CTF (**D**) bands (n=3) were quantified by densitometry and the relative densities were plotted.

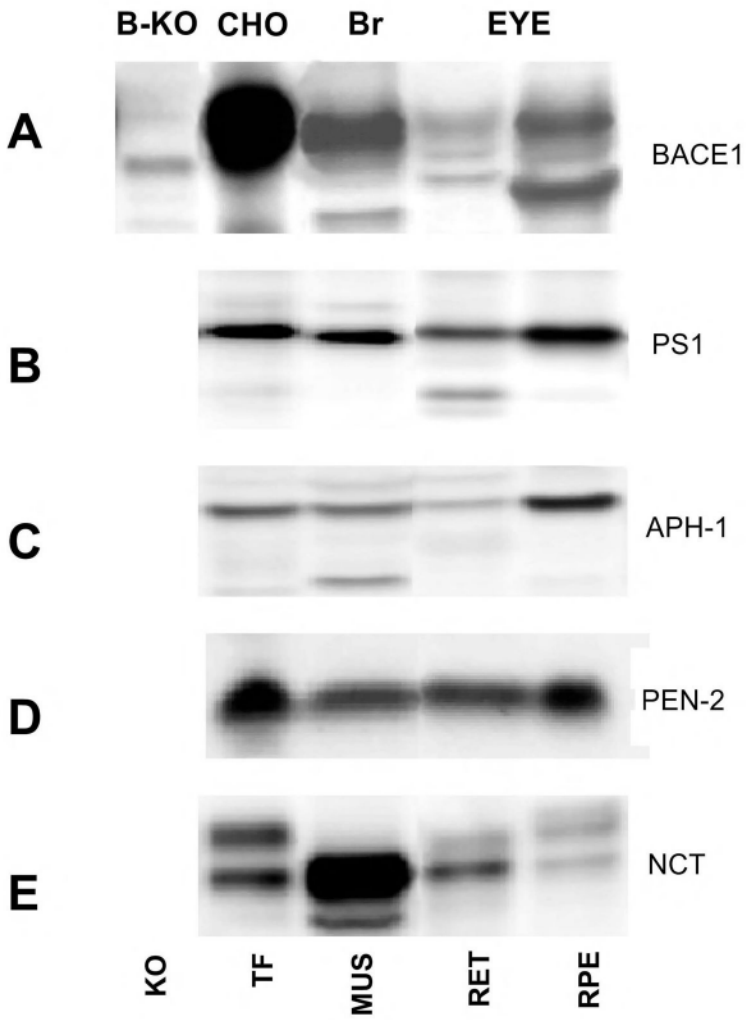

Figure 5. BACE-1 and γ-secretase subunits are expressed in the retina and RPE cell layers

BACE-1 (**A**), PS-1 (**B**), Aph-1 (**C**), Pen-2 (**D**), and nicastrin (NCT) (**E**) were analyzed in mouse (MUS), mouse retina (RET) and retinal pigment epithelium (RPE) cells. Transfected CHO cells (TF) were included as positive controls for all analyses and BACE-1 knockout (B-KO) mouse brain was also included for (**A**). BACE-1 and all γ-secretase subunits are expressed in the retina and RPE cells. Note that no knockout models exist for PS-1, Aph-1, Pen-2, and NCT.

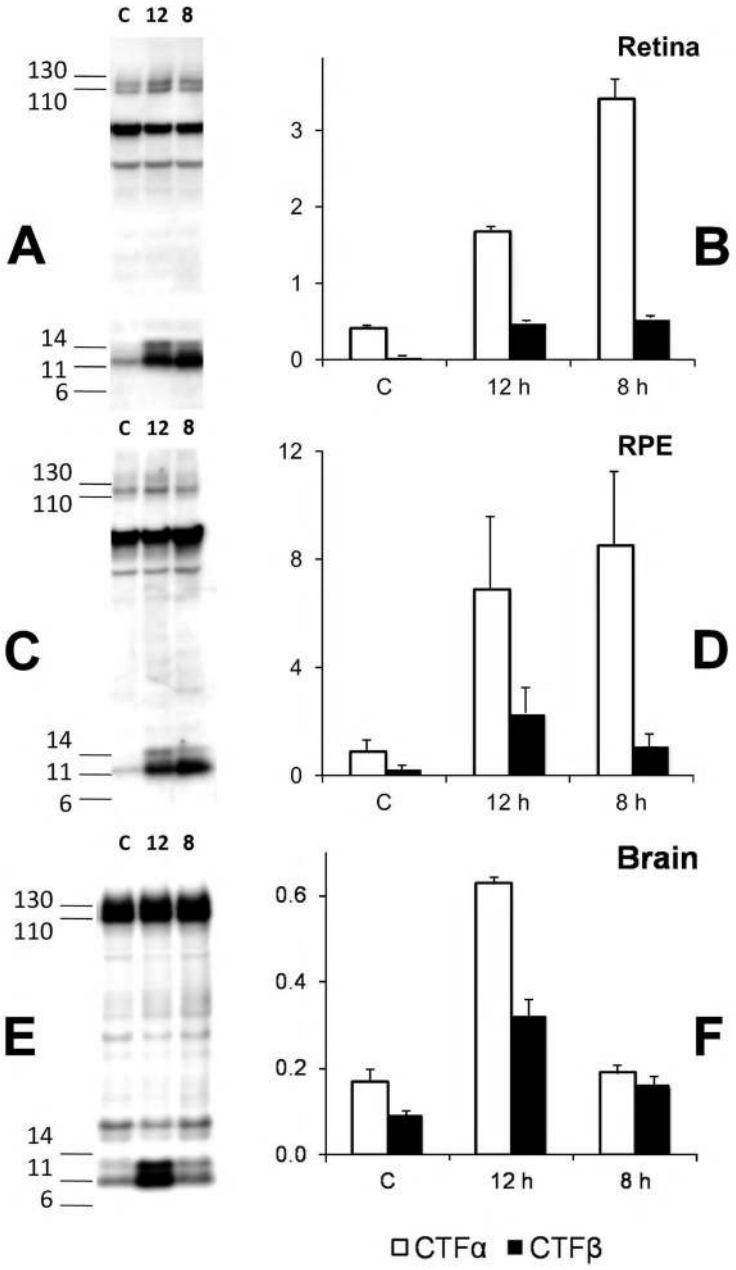

Figure 6. CTFα and CTFβ accumulate upon treatment with a γ-secretase inhibitor

YAC-AβPP transgenic mice (12–15 weeks of age) were administered saline (C) or the γ-secretase inhibitor LY411575 for 8 or 12 hours. Retina (RET, **A**–**B**), retinal pigment epithelium (RPE, **C**–**D**) and total brain (**E**–**F**) extracts from control and treated mice were analyzed by Western blotting with the O443 antibody. The bar graphs show a plot of the relative density (n=2) of CTFα and CTFβ bands after normalization to the full-length AβPP bands. With an n of 2, we are still able to see significant increases in CTFα and CTFβ after LY411575 treatment by ANOVA (Fisher's Protected Least Significant Difference (PLSD)) in the retina ($P<0.0001$) and RPE (CTFβ $P<0.01$; CTFα $P<0.0001$). Brain CTFβ was significantly increased ($P<0.01$) for 8 and 12 h but CTFα was significant only at 12 h).

CTFβ/CTFα ratio was highest in the brain (39±7%) but significantly lower in the retina (15±6%; P<1E-4) and RPE (19±6%, P<0.001).

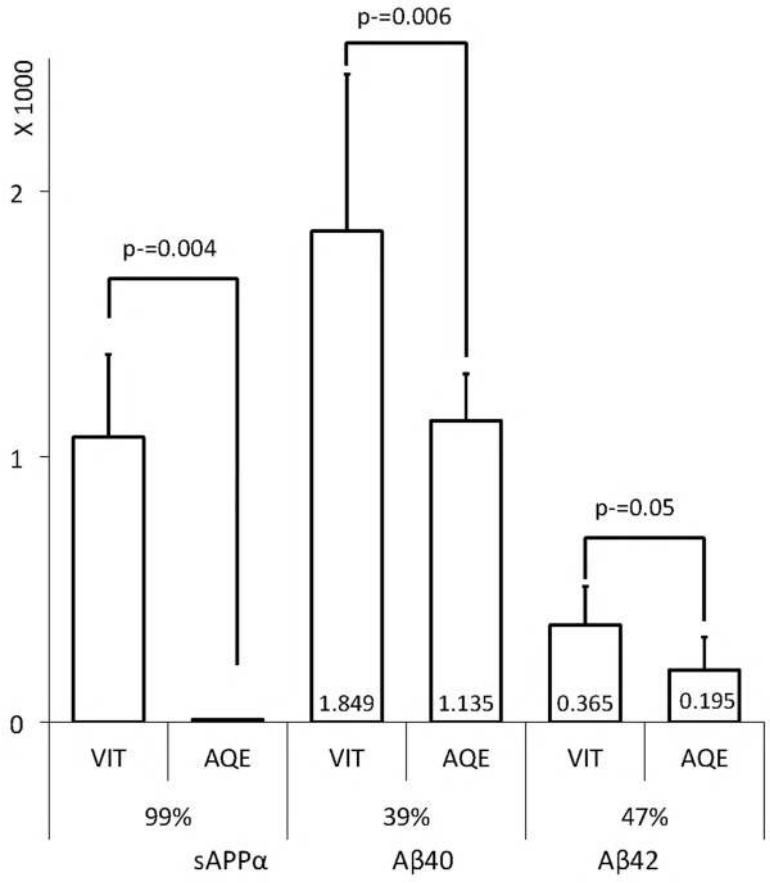

Figure 7. Relative Aβ and AβPP in bovine aqueous and vitreous humors

Vitreous (VIT) and Aqueous (AQE) humor levels of sAPPα (Relative band intensity) were determined by densitometry of Western blots (n=3). Aβ40 and Aβ42 levels (pM) were determined by ELISA after subtracting the background from peptide competition assays as described in the Materials and Methods section. The average Aβ levels are shown inside the bars (x 1000 pM). Note that when compared to the vitreous humor, 39–47% of Aβ40 (P=0.006) and Aβ42 (P=0.05) were recovered in the aqueous humor, but sAPPα levels drop precipitously by over 99% (P=0.004).